Effect of a Low-Rank Denoising Algorithm on Quantitative MRI-Based Measures of Liver Fat and Iron

Brian C Allen[1], Felix Lugauer[2], Dominik Nickel[2], Lubna Bhatti[1], Randa A Dafalla[1], Brian M Dale[3], Tracy A Jaffe[1], and Mustafa R Bashir[1,4]

[1]Radiology, Duke University Medical Center, Durham, NC, United States, [2]MR Application Predevelopment, Siemens Healthcare GmbH, Erlangen, Germany, [3]MR R&D Collaborations, Siemens Healthcare, Cary, NC, United States, [4]Center for Advanced Magnetic Resonance Development, Duke University Medical Center, Durham, NC, United States

Synopsis

Applying the described low-rank denoising algorithm to a liver fat/iron quantification technique reduces image noise in PDFF and R2* maps without adversely affecting mean values of the quantitative measures or reader assessment of edge sharpness.

Purpose

MRI-based measures of liver fat and iron are becoming widely available and clinically important for the assessment of fatty liver disease and iron deposition. Performing ROI-based measurements on quantitative proton density fat fraction (PDFF) and R2* maps can be challenging due to artifacts such as image noise, and noise can bias the PDFF and R2* measures themselves. Low-rank denoising is a method which has been described for reducing noise in image reconstructions based on multiple data sets which share similarities, and has been applied to PDFF measures obtained from six-echo gradient echo sequences (1). The purpose of this study is to assess the effect of a low-rank denoising algorithm on quantitative MRI-based measures of liver fat and iron, in terms of 1) PDFF values; 2) R2* values; 3) subjective image quality metrics.

Methods

This was an IRB-approved retrospective study. Raw data acquired from 44 consecutive subjects at 3T using a standard six-echo gradient echo sequence were reconstructed using a conventional magnitude image reconstruction, followed by the multi-step adaptive fitting algorithm to obtain PDFF and R2* maps (assuming the same R2* for fat and water); termed "original" maps (2,3). Then, a patch-wise low-rank denoising algorithm including automated noise adjustment was applied to the reconstructed complex-valued contrast images (1). This step is followed by the same reconstruction to obtain PDFF and R2* maps as before; termed "denoised" maps.

Pulse sequence parameters included: TR=8.9 ms; TE1=1.23 ms, with 6 echoes collected at ΔTE 1.23 ms; flip angle=4^{o}. PDFF and R2* maps were reconstructed along with goodness-of-fit (GOF) maps as previously described. Briefly, GOF was measured by using the PDFF and R2* maps to generate modeled 6-echo magnitude image sets, and the GOF was defined as the sum of squared residuals divided by the sum of squared data (4).

PDFF, R2*, and GOF maps were deidentified and randomized. For reader preference analysis, three readers compared original and denoised PDFF and R2* maps side-by-side, blinded to which image sets had been denoised. They recorded their preference for original vs. denoised maps in terms of vessel edge sharpness, liver edge sharpness, and image noise. After recording these preferences for all map pairs, these were de-randomized to yield a scale of: 1-strongly prefer denoised; 2-somewhat prefer denoised; 3-no preference; 4-somewhat prefer original; 5-strongly prefer original. An analysis of variance (ANOVA) was used to assess for differences from an overall value of 3 (no preference) for each visual assessment.

For quantitative analysis, an independent reader placed four regions of interest (ROIs) in the liver parenchyma, using the original TE=6.15 ms images, and copied these onto the PDFF, R2*, and GOF maps for both the original and denoised reconstructions. Mean and standard deviation of PDFF and R2* values were calculated. Agreement was assessed by intraclass correlation coefficients (ICCs). Differences between PDFF, R2*, and GOF values were compared between original and denoised maps using the Mann-Whitney-U test. Mean difference analysis was performed for PDFF and R2*.

Results

Representative PDFF and R2* maps are shown in Figures 1 and 2.

Reader preferences are summarized in Figure 3. 2/3 readers preferred vessel edge sharpness on the denoised maps ($p<0.001$-$p=0.57$); all three readers had no preference with regard to liver edge sharpness ($p=0.16$-0.48); all three readers preferred the

denoised maps with regard to image noise ($p<0.001$).

For quantitative analysis, agreement was near perfect between original and denoised maps for liver PDFF (ICC=0.995) and R2* (ICC=0.995). Liver PDFF was similar overall for original (7.6+/-7.2%) and denoised (7.7+/-7.7%, p=0.15), as was liver R2* (53.8+/-4 s^{-1} vs. 53.1+/-4.1 s^{-1}, p=0.11). GOF was improved for the denoised images (16.7+/-9.4 arbitrary units) compared with the original images (30.8+/-15.1 arbitrary units).

Mean difference between the techniques was -0.1+/-1.1% for PDFF and 0.8+/-5.6 s^{-1} for R2*.

Discussion

In this practical application of low-rank denoising, the mean values for the key quantitative measures PDFF and R2* were unchanged by application of the denoising algorithm, while goodness-of-fit to the signal model improved, as did reader impression of the images. Importantly, while image smoothing algorithms can blur edges, this denoising algorithm preserved or improved the visual impression of vessel and liver edges. This could, theoretically, facilitate ROI placement on clinical images.

Conclusion

Applying the described low-rank denoising algorithm to a liver fat/iron quantification technique reduces image noise in PDFF and R2* maps without adversely affecting mean values of the quantitative measures or reader assessment of edge sharpness.

Acknowledgements

No acknowledgement found.

References

1. Lugauer F, Nickel D, Wetzl J, Kannengiesser SA, Maier A, Hornegger J. Robust Spectral Denoising for Water-Fat Separation in Magnetic Resonance Imaging. In Medical Image Computing and Computer-Assisted Intervention–MICCAI 2015 (pp. 667-674).

2. Zhong X, Nickel MD, Kannengiesser SA, Dale BM, Kiefer B, Bashir MR. Liver fat quantification using a multi-step adaptive fitting approach with multi-echo GRE imaging. Magn Reson Med 2014;72(5):1353-1365.

3. Bashir MR, Zhong X, Nickel MD, Fananapazir G, Kannengiesser SA, Kiefer B, Dale BM. Quantification of hepatic steatosis with a multistep adaptive fitting MRI approach: prospective validation against MR spectroscopy. AJR Am J Roentgenol 2015;204(2):297-306.

4. Bacher MA, Zhong X, Dale BM, Nickel MD, Kiefer B, Bashir MR, Stollberger R, Kannengiesser SA. Signal model consistency analysis of different protocols and spectral models in multi gradient echo liver PDFF and R2* quantification. Preceedings of the ISMRM 2014; Milan, Italy.

Abstract ID: 5597

Figures

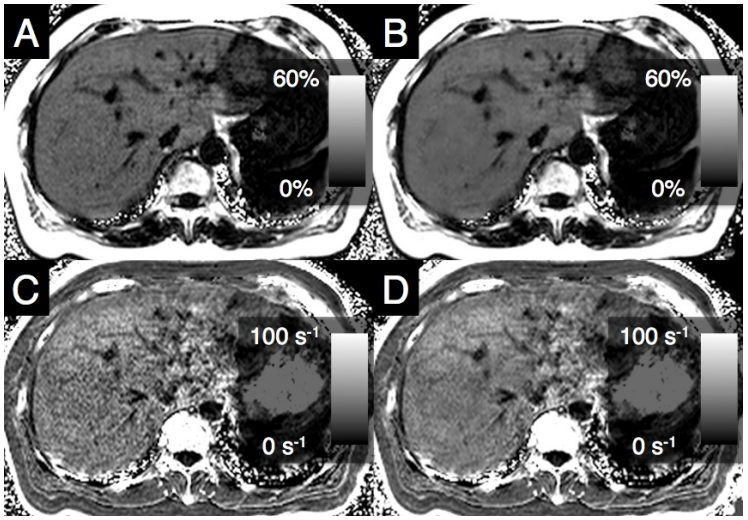

Figure 1: Representative images from a patient with a relatively high PDFF value of 23.7% and an R2* value of 47.4 s-1 on the original image reconstructions. (A) original PDFF map; (B) denoised PDFF map; (C) original R2* map; (D) denoised R2* map. Readers strongly the denoised images based on image noise.

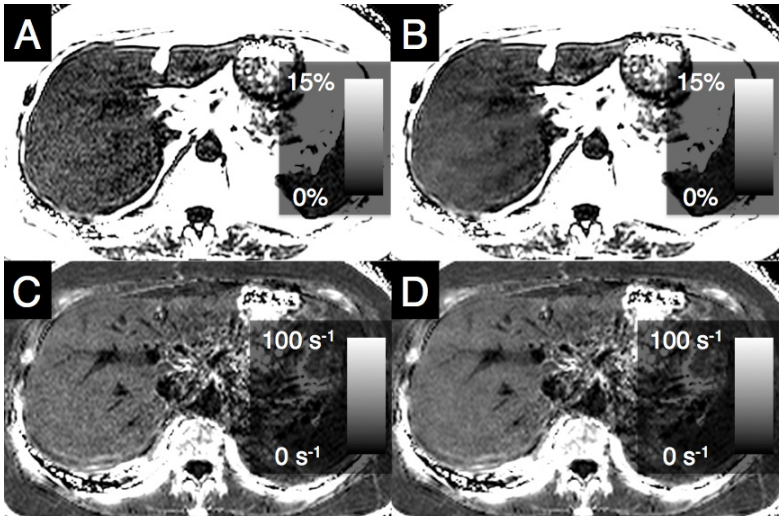

Figure 2: Representative images from a patient with a normal PDFF value of 4.6% and an R2* value of 42.4 s-1 on the original image reconstructions. (A) original PDFF map; (B) denoised PDFF map; (C) original R2* map; (D) denoised R2* map. Readers strongly the denoised images based on image noise and slightly preferred the denoised images based on vessel edge sharpness.

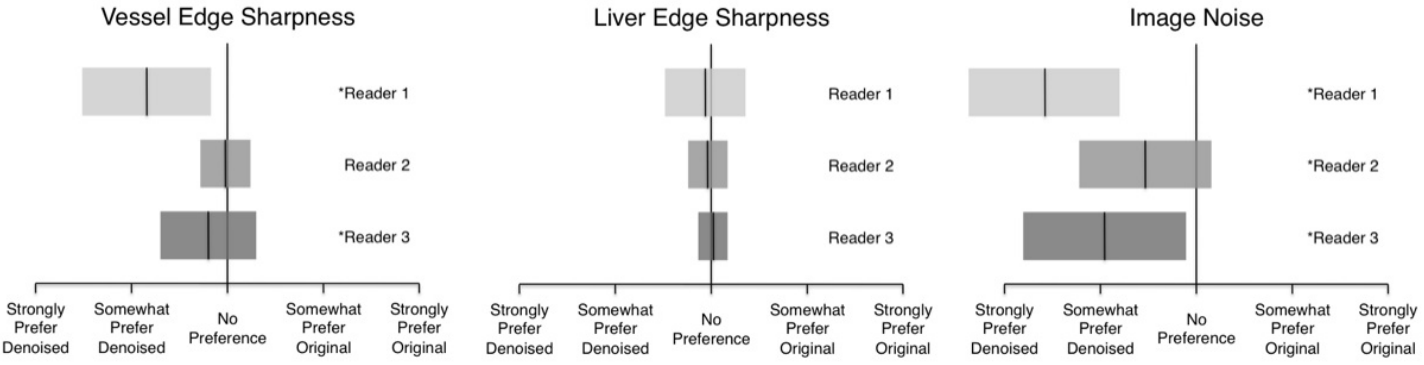

Figure 3: Summary of reader preferences for each of the three visual assessments performed in this study. * indicates statistically significant preferences for the denoised images for 2/3 readers based on vessel edge sharpness and all three readers based on image noise.